A digital version of Rossi's coincidence circuit

Marcello Carlà, Giacomo Poggi, Tommaso Righi and Samuele Straulino*
Department of Physics and Astronomy, University of Florence,
Via G. Sansone 1 50019 Sesto Fiorentino (FI), Italy
(Dated: July 1, 2026)

After more than a century since their discovery, cosmic rays remain a very active and fascinating research field and the coincidence method developed in those early studies is still a fundamental tool in experimental nuclear and particle physics. In this paper, Bruno Rossi's coincidence circuit, originally developed in 1930, is replaced by digital signal analysis of the outputs of three modern Geiger-Müller (GM) tubes. These tubes are conceptually similar to their historical counterparts, and their outputs are digitized using a computer sound card. The relation of coincidence rate to the thickness of overlying lead shielding, known as Rossi's curve, is reconstructed and compared with original historical data, the first experimental evidence of the electromagnetic showers. The digital implementation presented in this paper provides an effective and cheap educational tool for studying cosmic rays through signal coincidences using GM tubes and for approaching and deepening concepts that are still important in current physics research, like resolving time, and true and random coincidences. The total cost of the apparatus, including three detectors and the sound card, is around 1000 €.

I. INTRODUCTION

Rossi's coincidence circuit represents a milestone in the history of physics, particularly regarding the detection of cosmic rays. While working at the University of Florence, Rossi designed an experimental apparatus utilizing three Geiger-Müller tubes (described in Ref. 1) coupled to a circuit based on triode thermionic valves, the forerunners of the not yet invented transistor. This setup implemented in a very efficient way the 'coincidence method', invented by Bothe few years before: a pulse at the output of the circuit is produced only when all three GM tubes discharge simultaneously, providing a clear indication of the passage of an ionizing particle and strongly reducing the random combinatorial background.

In the present work, the signals from the GM tubes are digitized via a multi-channel sound card eliminating the need for a dedicated electronic coincidence circuit. We thoroughly discuss the system's resolving time and we quantify the various contributions to random coincidences. This work builds on inspiration from a previous project in which the output of the electronic coincidence circuit was digitized.[2]

Importantly, Rossi discovered that cosmic rays produce electromagnetic showers of secondary particles when passing through dense materials. This production of secondaries is represented by 'Rossi's curve', a graph relating the number of triple discharges to the thickness of the material above the detectors. Our apparatus reproduces this curve, and these results are compared with the original ones by Rossi.

Sec. II describes the Rossi coincidence circuit and its uses. We carefully discuss the definition of true and random coincidences as well as resolving time. Rossi's approach to estimating random coincidences and his famous curve are also presented. Sec. III describes our acquisition system and the associated off-line analysis of the digitized sequences. This analysis yields a timing 2-3 orders of magnitude better than what was possible with Rossi's circuit, thus rendering unnecessary the shielding against natural radioactivity that Rossi used to somewhat reduce random coincidences. Sec. IV describes in detail the method necessary for determining true coincidences and for categorizing and quantifying the random coincidences. In sec. V Rossi's curve is replicated with the new apparatus and dedicated software.

II. ROSSI'S COINCIDENCE CIRCUIT

A. The circuit

Bruno Rossi (1905-1993), while working as an assistant to Antonio Garbasso at the Physics Institute of the University of Florence in Arcetri (1928-1932), was deeply influenced by Bothe and Kolhörster's findings about the recently discovered cosmic rays and sought to extend their investigations.[3–6] For an overview of the early days of cosmic rays, which were fascinating the young Rossi, see the supplementary material. The most significant contribution by Rossi during this period was the development of the electronic coincidence circuit addressed in the present work. Unlike previous configurations, this novel design enabled the registration of simultaneous discharges across three or more detectors, generating a measurable output signal only when all units were fired concurrently – the actual meaning of the term concurrently will be explained (sec. II C) in terms of the system's resolving time.

In a seminal 1930 article – the source of the circuit diagram presented in Fig. 1 – Rossi described the operating principle of this device.[7] GM tubes are connected to the grids of three valves (A, B, C). A simultaneous discharge in all tubes interrupts the current in all three valves causing a sudden rise in the grid potential of valve D, whereas a discharge in only one or two tubes has little effect. The resulting variation of the anode current of valve D

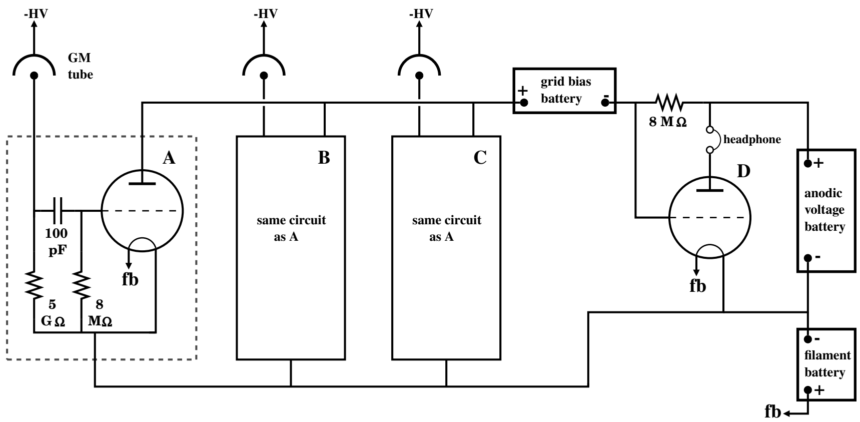

Figure 1. Schematics of Rossi's circuit redrawn from the original published in Ref. 7. The circuit is made of three identical paralleled sections (A, B, C) each one with a triode operating as a switch. Only when all three such switches do open by action of the GM tubes discharge, tube D generates a pulse in the headphone. The present drawing is meant to stress the structure which reminds the modern AND circuit.

is then detected by means of headphones. The advantage of this coincidence circuit with respect to Bothe's circuit for double coincidences is the intrinsic modularity of GM-triode chain, making it possible to easily extend the coincidence multiplicity. Noteworthy, Rossi's circuit represents the prototype of the future AND circuits.

B. Measurements performed by Rossi

Rossi arranged the Geiger-Müller tubes, connected to the coincidence circuit, in various geometric configurations. With three detectors aligned one above the other (Fig. 2-a), Rossi confirmed the existence of penetrating particles capable of traversing all three tubes.

Extending the pioneering work done by Bothe and Kolhörster, who utilized gold absorbers, Rossi inserted thick layers of lead between the tubes (Fig. 2-b). He verified that coincidences persisted even with a total shielding thickness of approximately 1 m of lead:

> I found that 60 per cent of the cosmic-ray particles capable of traversing 25 cm of lead also traversed 1 meter of lead.[3]

Each of these events was correctly attributed to the passage of a single, high-energy penetrating particle belonging to the so-called hard component of cosmic rays and later identified as a muon.

Rossi was forced to move the GM tubes farther apart than in the Bothe and Kolhörster configuration in order to provide room for very thick layers of lead, cheaper but less dense than gold. Actually Rossi was not interested in replicating the results of Bothe and Kolhörster, but he

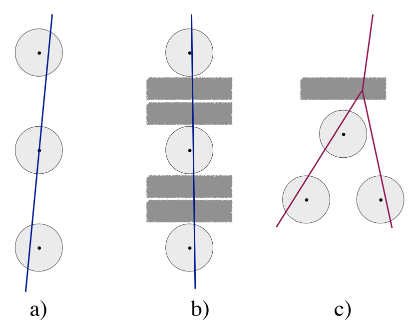

Figure 2. (Color online) Schematic showing different setups of GM tubes (circles), showing the path of a penetrating particle (blue line) and the development of an electromagnetic shower (red lines). (a) parallel tubes, (b) parallel tubes separated by lead absorbers (rectangles), (c) triangular tube arrangement with a lead layer above.

rather intended to find a limit to the penetrability of cosmic rays. The tubes were carefully aligned to track the straight-line trajectory of the candidate cosmic rays. As Bothe had already pointed out, when the counters are moved apart, an increasing fraction of events appears to derive from independent particles striking the tubes in rapid succession; Bothe called these events 'zufällige Koinzidenzen',[8] i.e. 'random coincidences', and Rossi adopted the same term.[9] The new three-fold coincidence circuit allowed for the fundamental reduction of the rate of random coincidences that would have rendered the experiment basically impossible for two counters separated by the same distance.

Using his circuit, Rossi observed unexpected events suggesting the production of secondary radiation in the surrounding shielding. To study this component Rossi arranged the tubes in a triangular configuration (like in Fig. 2-c), in which a single charged particle traveling in a straight line could not discharge all three tubes. The tubes were enclosed in a box made of thick layers of lead to shield them from the environmental radioactivity. The observed coincidence rate depended on the Pb thickness above the tubes. Upon removing the upper half of the shield, the rate dropped almost to zero, because a single particle could not satisfy the required coincidence condition, without the secondary particle production provided by the lead.

C. Rossi's curve and the estimate of random coincidences

After a few tests of this kind, Rossi published an article where he reported the rate of triple coincidences in a configuration similar to Fig. 2-c, while increasing the thickness of the upper part of the shielding, from zero up to several cm. He used layers of lead and iron and varied the distances between tubes and shielding. In Fig. 3 we only report the results referring to lead layers, extracted from the tables in Ref. 9. The two sets of data differ for the distance of the lead layer from the tubes. The number of coincidences per hour is represented on the y-axis. The inset shows the geometry of the used set-up. The behavior is similar for all the measurements; both lead curves show a peak for a thickness around 1.5 cm, while the iron curve (not shown) has a maximum at about 3 cm. The behavior of secondary emission intensity as a function of the lead thickness reported in Fig. 3 was soon christened Rossi's or shower curve.

As far as the physical process involved in Rossi's curve is concerned, it was soon recognized that an electromagnetic shower develops in the metal. This is a sprinkle of ejected electrons, positrons and photons following the interactions of similarly composed particles present in the cosmic rays (the so-called soft or electromagnetic component). These cosmic rays in turn mainly originate from the decay of neutral pions in the high atmosphere, and thus most of the observed secondary particles come from the upper part of the shield. The lower part, instead, serves to reduce the contribution from environmental radioactivity. Some of the secondary particles are detected as coincidences in the three tubes arranged in the triangular configuration. The presence of a maximum as a function of the absorber thickness is due to the increased probability of shower production with traversed material and to the competing increased absorption probability.

The original figure of Ref. 9 reporting these results contains curves through the points, intended only as guides for the eye. In fact, Rossi did not propose a specific an-

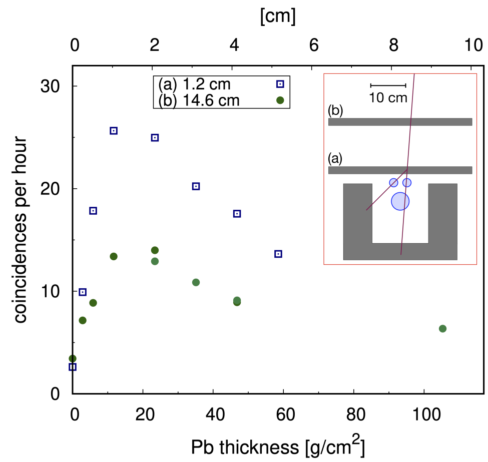

Figure 3. (Color online) Rossi's curve for lead layers, with data taken from tables of the 1933 article.[9] The used GM tube configuration, extracted from the same paper with added distance scale, is shown in the inset (see the original article for further details). Symbols report counts per hour as a function of the thickness of the lead layer placed above the tubes. The two sets of data correspond to distances of GM tubes from the lower lead layer of 1.2 cm (case a – open squares) and 14.6 cm (case b – filled points). A shower of secondary particles is sketched only for case (a).

alytical model for the newly observed and unexpected trend. Although the basic mechanism responsible for electromagnetic showers was soon identified by Rossi as the e^+/e^- production by high energy gamma rays and the following e^+/e^- interactions in the material, the accurate description of the curve shape required the knowledge of details, not easily available, like the energy spectra and the local composition of the soft component of cosmic rays. These complications are mentioned by Rossi himself in his book, published twenty years after discovery of the showers.[10] In the present days, very powerful simulation codes like Fluka[11] and Geant4[12] are typically used for reproducing and modeling also the experimental data on electromagnetic showers.

In Rossi's original report a detailed discussion is dedicated to the estimate of true and random coincidences, basing on the resolving time of the apparatus.[9] In fact, for any device devoted to determining whether the events of interest are simultaneous or not, the resolving time τ is defined as the largest time difference amongst the events within which they are considered simultaneous. If this condition is satisfied, the device is said to have detected a coincidence. Obviously, as far as τ is concerned, the smaller the better.

Since τ cannot be zero, this time interval might include both the truly time-related events emerging from a single physical process (true coincidences), and also independent events that have chance times of occurrence within τ (random coincidences). For example, in the configuration of Fig. 2-a a true coincidence corresponds to simultaneous discharges of the three GM tubes produced by a penetrating particle punching through all of them. In contrast, random coincidences are due to any combination of signals produced by natural radioactivity and/or cosmic rays, with two main different cases:

A) a true double coincidence of two tubes and an independent discharge on the third tube within τ;

B) three independent discharges on the GM tubes within τ.

Clearly, true and random coincidences cannot be distinguished, and only a statistical estimate of the two contributions is possible, once the value of τ is known.

In the simpler case of two detectors, the random coincidences rate ν_2 is found starting from the randomness and mutual independence of signals in the two detectors. Indicating with N_i the so-called rate of singles of the i–th detector, i.e. its counting rate due to both environmental radioactivity and cosmic rays, ν_2 is obtained from the number of signals on counter 2 falling within τ ($N_2\tau$) after a signal arrived in counter 1 (this happens N_1 times per second). Finally, the result is doubled because of the symmetric case that counter 2 precedes counter 1:

$$\nu_2(\tau) = 2\tau N_1 N_2 \tag{1}$$

The formula is valid under the assumption that both counting rates N_i are much smaller than $1/\tau$.

Rossi, aware that a direct estimate of τ would require detailed knowledge of the time dependence of the discharge, exploited Eq. 1 to derive τ from measurable quantities. The two GM tubes were placed far away from each other and in a skew relative geometry. The rate of singles N_1 and N_2 in each detector was measured; due to the statistical nature of radioactivity and cosmic rays, each counter registered a number of signals randomly distributed in time. The rate ν_2 of double coincidences was then measured using a relative geometry of the tubes for which the coincidences were purely random. The resolving time was thus determined from Eq. 1. Once determined, the value of τ does not depend on the set-up geometry provided that the circuit, the GM tubes and the applied high voltages are the same. For Rossi's apparatus, τ was in the range of 1 ms.

For estimating random coincidences in the set-up of Fig. 3 Rossi[9] generalized Eq. 1 to get the rate ν_3 of random coincidences for three detectors, taking into account the fact that the GM signals are basically all equal and the associated electronic chains are identical:

$$\nu_3(\tau) = 2\,\tau(n_{12}N_3+n_{23}N_1+n_{31}N_2) + 3\,\tau^2 N_1 N_2 N_3 \tag{2}$$

where N_i is the rate of singles of the i–th tube and n_{jk} denotes the rate of double coincidences between j–th and k–th tubes, all these rates being much smaller than $1/\tau$. The term linear with τ corresponds to case A) listed above, while the second term corresponds to case B). The rates of singles and of double coincidences are those measured in the operative conditions of the experiment; generally the last term in the sum is much smaller than the other ones. Having determined τ with the previous two-coincidence measurement, one can easily derive ν_3.

From Eq. 2 it is evident that in order to reduce the random coincidence rate, one can reduce either τ or the rates N_i and n_{jk}. To this aim, Rossi, having already optimized (and estimated) τ, introduced the heavy lead shielding around the counters (see the inset of Fig. 3) to reduce the counting rates N_i due to natural radioactivity. In fact the double coincidences n_{jk} are basically unaffected by the shielding, as they are caused by the penetrating component of cosmic rays. Basing on this procedure, Rossi found about 1-2 random coincidences per hour, for the experiment shown in Fig. 3. In the graph of the same figure the value of these random coincidences was not subtracted, but this did not affect the interesting part of the message, namely the presence of the maximum, that is not altered by any minor offset due to random coincidences.

In Eq. 1 and 2 the resolving time appears, which has a definition closely connected to the characteristics and/or limits of the used coincidence circuit. However, also in view of the following discussion, we stress that those two equations obviously apply to any interval of time θ, provided that its value satisfies the conditions for singles and double coincidence rates ($N_i \ll \theta^{-1}$ and $n_{jk} \ll \theta^{-1}$).

III. THE NEW ACQUISITION SYSTEM

A. Coincidence detection using a computer and a sound card

After the significant development of digital electronics in the last decades, the current trend in pulse detection and analysis is towards digitizing the signal as soon as possible after the minimal required analog processing, deferring the true pulse identification to a later stage, 'in software', through the numerical elaboration of the acquired samples.

In this experiment, we use GM tubes VacuTec model 70031 A, operating at a bias voltage of 450 V. The pulses typically have amplitude $\simeq -6$ V; rise time $\simeq 150$ µs; fall time $\simeq 500$ µs; overall length $\simeq 1$ ms; average repetition rate $\simeq$ 3 pulses/s, when the tube is exposed to the natural background. The effective length and diameter of the cylindrical tube are 230 mm and 18 mm, respectively (see the supplementary material for more details).

From these characteristics it is clear that all the frequency components of the signals fall inside the audio band, so that a medium quality PC audio board would be an adequate ADC. We choose the USB connected U-Phoria UMC404HD by Behringer as a good compromise among price and performances. All the four channels of the board can operate at the maximum sampling rate of 192 kHz, with a 24 bit resolution. Hence, each pulse from a GM tube can be acquired in a sequence of a few hundred samples. Measurements on the board gave an overall dynamic range of 10^4, corresponding to the ratio between the full scale of the ADC and the noise floor.

The only piece of analog electronics required between the GM tubes and the audio board is an adapter from the high impedance typical of the GM circuit (1 MΩ) to the 10 kΩ input impedance of the audio board (see the supplementary material for schematics and further details).

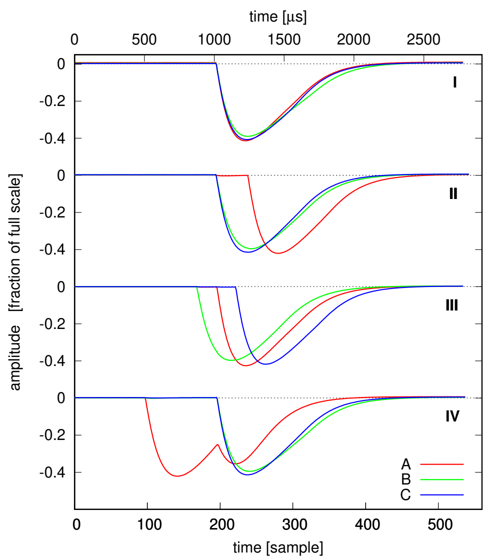

Figure 4. (Color online) Signals acquired by the audio board from three GM tubes. The sampling rate is 192 kHz and the ADC resolution is 24-bit. Signal amplitude is given as fraction of full scale (15 V). Panel I: all the three tubes discharge within a very short time interval, less than one sample long. Typically such an event corresponds to a triple coincidence, as defined in sec. II C. Panel II: a double coincidence on channels B and C, followed by an isolated event on channel A. Panel III: three isolated signals separated by approximately 25 samples (∼130 µs). Panel IV: an isolated signal from tube A, followed by a true triple coincidence, occurring on the tail of the first signal; the offline data analysis is capable to correctly disentangle the two events also in spite of the fact that the amplitude of the second piled-up signal partly suffers of a delay from the first event shorter than the recovery time of the GM tube.[1] The pre- and post-trigger guard segments are 200 samples long.

The plots in Fig. 4 show the shape of the pulses from the GM tubes and three typical timing cases. In panel I, we have a triple coincidence, as defined in sec. II C. It can be a single particle traveling through three parallel and vertically mounted tubes or a shower that simultaneously hits three tubes arranged in a triangular configuration. Since the speed of cosmic rays is very close to that of light, delays due to the centimeter-scale distance among the tubes are in the nanosecond range. The time spread in the signals of GM tubes is due to the electron drift time before the discharge sets in and falls in the 1 µs range. Hence such an event is characterized by the presence of three pulses that start together in a very tight time window, provided that the electronics of the three channels and the cable lengths are strictly matched.

In panel II, only tubes B and C show signals very close in time, while tube A discharges about 45 samples (230 µs) later: this can be due to a single particle that has crossed tubes B and C producing a double coincidence, while tube A has independently fired a little later by another particle. This corresponds to case A) of sec. II C.

The plot in panel III shows three independent pulses spaced by approximately 130 µs, originating from three independent particles, of either cosmic rays or environmental radioactivity. This corresponds to case B) of sec. II C. Using these digitized signals, it is possible to clearly identify with great accuracy the three cases. The same task was not possible for Rossi's circuit: it could only detect the overlapping among the signals, that in these three cases occurs in a similar extent.

The last plot, in panel IV, shows a true triple coincidence with the pulse from tube A piled-up with a previous independent event from the same tube.

Data was acquired using a program (`event_logger`) described in detail in the supplementary material. The main feature of the program is a selective coarse trigger that allows to accept/reject data on the basis of a signal presence in the channels, according to a given logical pattern: a signal on channels A and B or a signal on channels A, B and C, etc. A signal is considered present in a channel as long as its level satisfies a given predefined threshold of typically 10% of full scale.

Data selected by this acceptance trigger, including a guard segment of pre- and post- trigger data, are saved to disk for further offline analysis, together with the local time and the used selection pattern. Typically, pre- and post-trigger lengths are from 20 to 200 samples. Working conditions similar to Rossi's coincidence circuit can be obtained using the pattern 'A&B&C'. Yet, all cases reported in Fig. 4 are compatible with this pattern; only the following off line data analysis makes it possible to identify the true triple coincidence on the basis of the measured time differences between signals (panels I and IV), rejecting the other two combinations (panels II and III).

Another useful trigger pattern is '(A&B) | (B&C) | (C&A)'. In this condition, Rossi's triple coincidences are only a small subset of all recorded events and the other events may help to better understand the behavior of the system. Indeed, this trigger pattern was used for acquiring all the data presented in the following; it allowed, thanks to the guard samples and to the inclusion of double coincidences, determination of random coincidences over an extended range of time differences (see sec. IV B) and comparison with the estimate of Eq. 2 (see sec. V).

B. Offline data analysis

A first step of the offline analysis performs the timing, i.e. identifies, as accurately as possible, the exact time of occurrence of the event that generated the signal in the examined GM tube X, in the following indicated as T_X and referred to as time mark.

In recent decades, the timing of fast detector signals is performed using the 'constant fraction' technique[13], more recently in its digital implementation (see for example Ref. 14). However, given the characteristics of the signals of our tubes and their fairly constant amplitude and shape, a simpler and more rudimental technique could give equivalent or even better results. Observing the magnitude of the signal in Fig. 4, it is clear that the point where the slope changes abruptly from the base line into the fast rising front edge, as illustrated in Fig. 5, gives the time mark to a great accuracy. Further details of the algorithm used are described in the supplementary material.

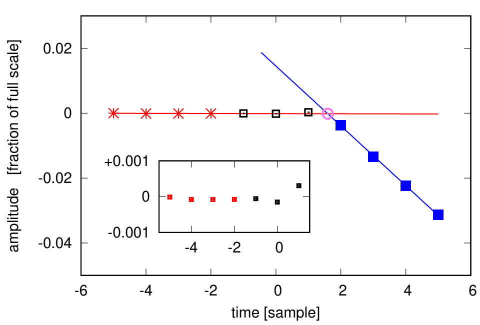

Figure 5. (Color online) Determination of the starting time of a pulse. From left to right, there are four points from the baseline (red stars), three unused points (black boxes) and four points from the rising edge of the pulse (blue squares). The red and blue lines are from a linear fit of first and last four points. The point where the lines intersect, marked with a violet circle, is taken as the time mark of the signal. The red and black small squares shown in the left-bottom inset repeat the corresponding red and black points, with a y-scale magnified by a factor of about 10. This makes clearly visible a disturbance that affects the points immediately before the signal rising front: this is discussed in the supplementary material.

Another noteworthy feature of this digital technique is its capability of disentangling piled-up pulses; that is, to detect a second pulse that starts on the tail of a previous one, as in the case of panel IV of Fig. 4. The time mark resolution obtained with the outlined procedure falls in the order of a few hundreds of ns, as shown in the next section.

The simplicity of this analysis makes it a good subject for a student programming exercise.

IV. DIGITAL IMPLEMENTATION AND COINCIDENCES

A. Resolving time, true and random coincidences in our digital approach

In this section, the new software procedure to analyze the digitized sequences is described. In this context the concept of resolving time is revisited and partly updated.

Since one of the main issues in a coincidence experiment is the reduction of random coincidences described by Eq. 2 for the case study of three detectors, we anticipate that in our digital approach such a reduction is successfully achieved by significantly reducing the resolving time τ and not by adding lead shielding around and below the GM tubes, as Rossi was forced to do. Therefore, the following discussion proceeds by stressing similarities and differences with respect to Rossi's approach.

The coarse acceptance trigger introduced in sec. III is conceptually similar to the behavior of Rossi's circuit. In fact, if we perform a triple coincidence run with a 'A&B&C' trigger pattern, the time spent by any signal above the coarse-trigger threshold represents a time interval within which the other two signals have to appear; therefore this 'time over threshold' basically acts as the resolving time of Rossi's circuit. A similar consideration applies when triple coincidences are collected by using the trigger pattern '(A&B) | (B&C) | (C&A)'. For this reason this time will be referred to as trigger-related resolving time τ_{tr}.

For a triple coincidence run, after having determined the accurate time marks T_A, T_B, T_C for the three GM tubes, a second step of the offline analysis consists of selecting events with θ such that $|t_{ab}|, |t_{bc}|, |t_{ca}| \leq \theta$. This is always possible, as long as $\theta \leq \tau_{tr}$.

In panel (a) of Fig. 6 we report a two dimensional histogram containing the correlation between $t_{ab} = T_A - T_B$ and $t_{bc} = T_B - T_C$, within a time range of 1.2 ms. This kind of correlation contains all the information regarding the examined coincidences, because the time-mark differences between the three tubes are not independent:

$$t_{ab} + t_{bc} + t_{ca} = T_A - T_B + T_B - T_C + T_C - T_A = 0\ . \quad (3)$$

For this reason, the following analysis can be done by considering any combination of pairs of tubes.

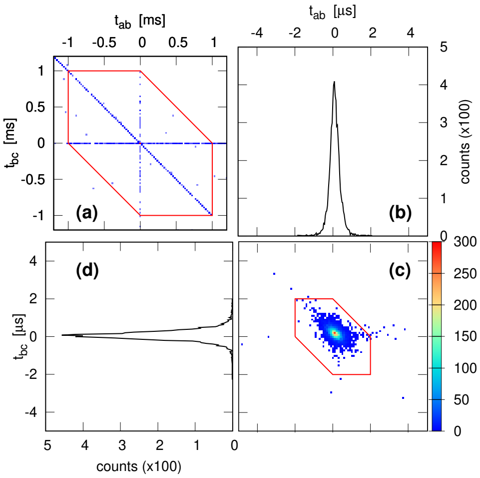

Figure 6. (Color online) Panel (a): correlation between the time difference of tubes A and B (t_{ab}) and that of tubes B and C (t_{bc}) over the full range of time acquisition. The correlation is reported as a two-dimensional histogram. The thick red line defines the contour corresponding to $\theta = 1$ ms (see text). Panel (c): the same as in panel (a), but for a narrower region on both axes. The thick red line defines the contour corresponding to $\theta = 2\,\mu$s. The time scales of the X and Y axis of this panel are those reported in the projections shown in panel (b) and (d), respectively. Panel (b): projection over the t_{ab} axis of the contents inside the region of the histogram shown in panel (c). Panel (d): projection over the t_{bc} axis of the contents inside the region of the histogram shown in panel (c). Data correspond to the 5-th row of Tab. I (sec. V).

To see the region where the events selected by a chosen time-window lie, in the same panel (a) of Fig. 6 a thick red line represents, as an example, the contour including the events corresponding to a selection of $\theta = 1$ ms. The non obvious hexagonal shape of the contour depends on the condition expressed by Eq. 3; namely the slanted lines correspond to the limit imposed on the third, not seen difference: $|t_{ca}| = |-t_{ab} - t_{bc}| \leq \theta$.

A narrow peak stands up at (0,0) in the histogram of panel (a) of Fig. 6, though hard to identify because of the wide time range of the plot. The presence of the peak can be appreciated in panel (c). This peak clearly identifies the true coincidences between tubes A, B and C amongst the whole set of examined time differences. In this panel the thick red line represents the region mapped by a time window $\theta = 2\,\mu$s. The non-zero and negative correlation coefficient in the two-dimensional histogram of panel (c) is obviously due to the presence on both axes of the time of tube B, with opposite sign.

Visible – though small – offsets with respect to zero are present, presumably due to the non perfect clock synchronization of the channels of the sound card and/or to the slightly different time response of the GM tubes. In spite of these offsets, which can be easily corrected for during the analysis, the peak along the two axes is about 2 μs wide at its base, as can be seen in panels (b) and (d), containing the projections on the t_{ab} and t_{bc} axes of the events enclosed in the relevant time-window. Both peaks have rms widths $\sigma \approx 0.3\,\mu$s. An almost identical distribution is obtained for the time differences between GM tubes C and A, not shown. This sub-μs rms value is close to the limit imposed by the time-response of the GM tubes.

In this triple coincidence experiment, the width at the base of the peaks is basically the minimum time-differences which can be experimentally identified, satisfying the coincidence requirement for the three signals. Therefore a time window $\theta = 2\,\mu$s can be interpreted as the resolving time τ_{dp} attainable with our approach, the subscript reminding the 'digital procedure' needed to determine it. This resolving time is over two orders of magnitude smaller than τ_{tr} which is close to that of Rossi's circuit. Of course, this result simply benefits of the technological progresses emerged during the about 100 years after the introduction of Rossi's circuit.

B. Random coincidence pattern

Outside the peak region only random coincidences appear. According to the point addressed in sec. II C about the applicability of Eq. 2 to any small interval of time, the hexagonal regions mapped by θ in the two-dimensional histograms of Fig. 6 do contain a number of random coincidences proportional to $\nu_3(\theta)$.

A closer look to the pattern of residual counts far from the central ones is visible in panel a) of Fig. 6. The intensification of counts along three lines going through the origin correspond to the terms of Eq. 2 linear in τ (in θ in the present context). The points lying on the y-axis correspond to a true double coincidence between A and B tubes with $t_{ab} \approx 0$, accompanied by a random walking tube C. Similar feature is for the counts lying on the x-line: true coincidence between tubes B and C, with a random walking A. The diagonal line is now easily attributed to true coincidences between tubes A and C, accompanied by a random walking B; in fact, counts around the line $t_{bc} = -t_{ab}$ have coordinates satisfying the condition $t_{ab} + t_{bc} = -t_{ca} \approx 0$.

The last contribution to random coincidences in Eq. 2, now depending quadratically on θ, is associated with the background of counts, sparse and barely visible because very rare, lying everywhere in the two-dimensional histogram without any specific pattern.

The possibility of identifying the various contributions to random coincidences is interesting from the educational point of view and gives the opportunity to evaluate their amount experimentally, too. First of all, one verifies the expected uniformity of their distribution. This

Table I. Sequence of measurements for reproducing Rossi's curve ($\mathcal{C}$ = coincidences).

Pb layer [cm]	Time [h]	True $\mathcal{C}$ $\theta = 2\,\mu\mathrm{s}$	Total $\theta = 1\,\mathrm{ms}$	True $\mathcal{C}$ rate [h^{-1}]	Random rate [h^{-1}]
0	382	2949	5042	7.7 ± 0.1	0.011
0.22	46	998	1252	21.7 ± 0.7	0.011
0.6	46	1614	1846	35.1 ± 0.9	0.010
1.0	53	2315	2575	43.7 ± 0.9	0.010
1.8	142	5512	6149	38.8 ± 0.5	0.009
3.0	46	1393	1611	30.2 ± 0.8	0.009
4.0	69	1692	1970	24.5 ± 0.6	0.008
5.0	46	1003	1170	21.8 ± 0.7	0.007
9.1	44	866	1038	19.7 ± 0.7	0.008

can be qualitatively appreciated by simple inspection of the histograms of panel (a) in Fig. 6. More accurately, by varying θ in the software procedure, it is possible to study the dependence of the number of selected events as a function of θ, effectively acting as τ in Eq. 2: a linear dependence on θ, due to the negligibly small contribution of the last term of Eq. 2 is indeed easily observed. Having verified this, a simple method appears for determining the amount or random coincidences buried under the true coincidence peak. In fact, with direct reference to the regions mapped by θ in panels (a) and (c) of Fig. 6, the difference between the number of coincidences observed for $\theta = 1000\,\mu\mathrm{s}$ and those for $\theta = 2\,\mu\mathrm{s}$ provides the number of pure random coincidences outside the peak region. Therefore this amount, scaled by a factor $2\,\mu\mathrm{s}/(1000-2)\,\mu\mathrm{s} \approx 2\cdot10^{-3}$, gives directly the number of random coincidences under the peak region. In the next section, the procedures illustrated in this section, including the one for determining random coincidences, will be applied for a replication of Rossi's curve.

V. MEASUREMENTS ON COSMIC-RAY SHOWERS AND ROSSI'S CURVE

Applying the described acquisition system and analysis procedures, we performed measurements in a set-up (Fig. 7) similar to that described by Rossi, with the triangular arrangement of the detectors. We added in steps sheets of lead above the tubes.

The sequence of measurements is summarized in Tab. I. For each lead layer placed above the tubes, the table reports the measurement duration, the number of triple coincidences within the $\pm 2\,\mu\mathrm{s}$ peak window (our τ_{dp}), the total number of events within ± 1 ms range (a value close to the resolving time of Rossi's circuit), the rate of true coincidences per hour, including its associated statistical uncertainty, and the rate of random coincidences under the peak. As Tab. I shows, this kind of measurements requires exposure time long enough to achieve the small error reported in the fifth column.

Results shown in Fig. 8 show a behavior similar to those reported by Rossi in Fig. 6.7.1 of his book "High-energy particles"[10], published twenty years after his discovery of showers and reported as squares in the same figure. Data presented in the book extended the set of measurements for lead layers placed at a distance of 1.2 cm above the GM tubes already present in Fig. 3. In fact, the new graph, while containing the same results of Fig. 3 for lead thickness smaller than 100 g/cm^2, adds information about coincidence rates registered for thicker layers showing the flattening of the curve also evident in our data in Fig. 8.

Figure 7. (Color online) A photo of the GM arrangement used to reproduce Rossi's curve. The tubes are kept on the vertices of an equilateral triangle with a side length of 40 mm thanks to properly machined plastic spacers inserted between them. Lead sheets (for a total thickness of 91 mm in this case) were placed horizontally above the tubes, as shown, resting them on lateral supports made of wood.

The lead thickness corresponding to the maximum rate of our and Rossi's data are consistent. In fact, as already discussed in sec. II C, the maximum position resulting from the competing effects of production and attenuation of electromagnetic particles depends only on the electromagnetic component of cosmic rays and on the nature of the absorbing material. The differences of our and Rossi's set-up are responsible for absolute rates which in our case, for all lead thicknesses, including the no-lead one, are significantly higher than those reported by Rossi. The possible origin of the observed differences in the coincidence rates are briefly discussed in the supplementary material.

We have already shown that the background of random coincidences, already small in Rossi's experiment (1-2 per hour), is basically negligible in our case. Quantitatively,

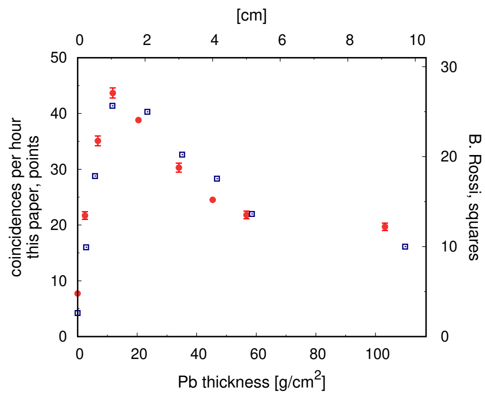

Figure 8. (Color online) Points represent Rossi's curve obtained with our apparatus. Squares are Rossi's data, published in Ref. 9 and coinciding with those of Fig. 3, apart from later added rightmost point[10].

using the procedure described before, we measure a random coincidence rate under the peak of true coincidences of about 10^{-2} per hour, about two orders of magnitude smaller than that reported by Rossi. This is not surprising, because our effective resolving time, over two orders of magnitude smaller than Rossi's, largely compensates for the increased random coincidences – at most a factor of two – due to the absence of the lead shield. For each measurement reported in Tab. I, a short run was performed to determine the rate of singles. This has been done by using as a trigger pattern the OR of the three tubes 'A | B | C'. For each measurement, the experimentally determined coincidence rate agrees with the corresponding estimate of Eq. 2 within the expected uncertainties. These uncertainties are determined by standard error propagation of the involved counts assuming for them a standard deviation equal to their square root, i.e pure Poissonian fluctuations, and a negligible error for the time duration.

VI. CONCLUSIONS

The digital implementation presented in this paper provides instructors with a highly accessible, low-cost bridge between historical milestone experiments and modern digital data acquisition techniques.

The tubes can be arranged in an aligned configuration – vertically stacked – to study the rate of the hard component of cosmic rays, or in the triangular configuration pioneered by Rossi to detect showers generated by the soft component. Throughout this study, we have discussed random coincidences in detail, evaluating their specific contribution to measurements. Furthermore, we retraced the fundamental steps required to obtain Rossi's curve, comparing our experimental results with original historical data. We believe that performing these experiments, and in particular the replica of Rossi's curve, could be very useful for college students. The equipment is relatively simple and cheap, but it has to be built by the experimenters and it cannot be simply ordered as a black-box from an on-line store. This helps significantly to understand the experimental procedure and the associated physics.

Finally, we suggest interesting aspects of triple coincidence measurements which might be deepened with the digital implementation, namely:

a) The effect on the coincidence efficiency associated to the dead time of GM tubes, which hinders any response to a second ionization following a previous one within a few hundreds of µs. This can be done by placing in the vicinity of the tube an even weak radioactive source to increase the rate of singles.

b) The way of determining the efficiency of the GM tubes via triple coincidences.

c) The effect on timing due to the electron drift inside the GM tubes, which can be approached via controlled misalignment of the tubes and accurate timing of the so-enhanced fringing tracks.

AUTHORS DECLARATION

M. Carlà designed the electronic interfaces for the sound card, developed and refined the data acquisition software. G. Poggi supervised the data analysis, drafted the manuscript sections on true and random coincidences and proposed criteria for an efficient rejection of random coincidences. T. Righi, a physics student preparing his final dissertation, contributed significantly to the preliminary data acquisition and analysis. S. Straulino coordinated the whole research, collected final data and was responsible for the historical context. All authors contributed to the review of the manuscript and approved the final version.

Conflict of Interest: the authors have no conflicts to disclose.

* samuele.straulino@unifi.it

[1] Knoll, G.F. (2015) Radiation Detection and Measurement

(fourth edition). New York: John Wiley & Sons

[2] Carlà, M., Giatti, A., Poggi, G. and Straulino, S. 'Rossi's coincidence circuit: a reconstruction for educational purposes, with period instruments', Proceedings of the SISFA 42nd Annual Conference, edited by Bussotti, P., Capecchi, D. and Tucci, P., DOI: 10.12871/978883339843330

[3] Rossi, B. (1964). Cosmic Rays. New York: McGraw-Hill

[4] Bonolis, L., 'Walther Bothe and Bruno Rossi: The birth and development of coincidence methods in cosmic-ray physics", Am. J. Phys. 79 (2011), 1133-1150.

[5] Leone, M., Mastroianni, A. and Robotti, N., 'Bruno Rossi and the introduction of the Geiger-Müller counter in Italian physics: 1929-1934', Physis, 42 (2005), 453-480.

[6] Peruzzi, G. and Talas, S., 'The Italian contributions to cosmic-ray physics from Bruno Rossi to the G-Stack. A new window into the inexhaustible wealth of nature', Riv. Nuovo Cim. 30 N. 5 (2007), 197

[7] Rossi, B. (1930). 'Method of Registering Multiple Simultaneous Impulses of Several Geiger's Counters', Nature, 125, 636.

[8] Bothe, W., Kolhörster, W. 'Das Wesen der Höhenstrahlung', Z. Physik 56, 751–777 (1929). https://doi.org/10.1007/BF01340137

[9] Rossi, B. (1933). 'Über die Eigenschaften der durchdringenden Korpuskularstrahlung im Meeresniveau (About the properties of the penetrating corpuscular radiation at sea level)', Zeitschrift für Physik 82, 151–178.

[10] Rossi, B. (1952). High-Energy Particles. New York: Prentice-Hall, p. 319

[11] See `https://fluka.cern/`

[12] See `https://geant4.web.cern.ch/`

[13] Gedcke, D.A. and McDonald, W.J., 'A constant fraction of pulse height trigger for optimum time resolution', Nuclear Instruments and Methods 55 (1967) 377–380

[14] Bardelli, L., Poggi, G., Bini, M., Pasquali, G. and Taccetti, N. 'Time measurements by means of digital sampling techniques: a study case of 100 ps FWHM time resolution with a 100 MSample/s, 12 bit digitizer', Nuclear Instruments and Methods in Physics Research A 521 (2004) 480–492